

Assessment of Gas-Slag-Metal Interaction During a Converter Steelmaking Process

Lingling Cao, Yannan Wang, Qing Liu, Lefei Sun, Sangsang Liao, Weida Guo, Keshe Ren, Bart Blanpain and Muxing Guo

Abstract The interaction between a supersonic oxygen jet and liquid metal is a dominant factor affecting transport phenomena during the converter process. A systematic description of the interaction is of significant importance for a quantitative understanding of the transport phenomena. In this paper, cold model experiments and the corresponding numerical simulations were carried out to investigate the gas-slag-metal interaction inside an 80 t BOF converter. The effects of the operation parameters, such as inlet pressure, slag thickness and slag viscosity on the multiphase interaction have been studied. It has been found that the cavity profile is closely related to the operational conditions. The cavity depth increases with an increase in oxygen inlet pressure, whereas the cavity width is much less affected. The cavity profile is also clearly influenced by the thickness of the slag layer. The influence of slag viscosity on cavity profile is not significant under the present simulation conditions.

Keywords Gas-slag-metal interaction · Cavity shape · Operational condition
Slag property · BOF steelmaking

L. Cao · Q. Liu (✉)
State Key Laboratory of Advanced Metallurgy,
University of Science and Technology Beijing, 100083 Beijing, China
e-mail: qliu@ustb.edu.cn

L. Cao · Y. Wang · B. Blanpain · M. Guo
Department of Materials Engineering, KU Leuven, 3001 Louvain, Belgium

L. Sun · S. Liao
Xinyu Iron and Steel Group Co. Ltd, 338001 Jiangxi, China

W. Guo · K. Ren
Laiwu Steelmaking Plant, Shandong Iron and Steel Group, 271126 Shandong, China

Introduction

The Basic Oxygen Furnace (BOF) steelmaking process can rapidly refine molten iron and scrap into liquid steel with a desired carbon content and temperature via the top injection of high pressure oxygen gas jet. The interaction between gas and liquid metal/slag is the primary determinant of all the complicated phenomena during the converter process [1]. For instance, the top blown jet can affect the decarburization rate and the total Fe content in the slag at the final stage of the process. Therefore, a systematical description of the interaction could be conducive to clearly understand the highly coupled transport phenomena inside the converter, and to further achieve the development of fundamental insights, process optimization [2] and end-point control of BOF operations [3].

Due to the fairly sophisticated transport phenomena and the difficulties in direct observation, water modeling coupled with mathematical modeling offers important tools for tackling process development and optimizing the BOF steelmaking process [4]. Sharma et al. [5] found that the shape of the cavity caused by gas impingement can be predicted from dynamically scaled water models. Molly [6] identified three interaction types as dimpling mode, splashing mode and penetrating mode according to the geometrical shape of cavity. Nordquist et al. [7] studied the effects of nozzle diameter, lance height and gas flow rate on the penetration depth in a water model during the blowing process. It was proved that the penetration depth increased with an increased jet momentum number. Odenthal et al. [8] numerically simulated the penetration of the supersonic oxygen jets and the motion of the phase interfaces. The CFD model was used to gain a better insight into the melt flow related phenomena. Li et al. [9] studied the interaction behavior between the high speed oxygen jet and steel bath under steelmaking conditions in a commercial 150-ton converter. Simulation results showed that the operating pressure of oxygen jet has a much more significant impact on the behavior of slag-metal interface compared to the surface tension of the melts. Sabah et al. [10] presented a novel approach and identified various cavity modes by analyzing the sound produced in the bath. Understanding the interaction would be potentially beneficial to control splashing and prevent slopping. Besides, the interaction is believed to be closely related to actual production [11, 12], e.g. decarburization and dephosphorization process. According to the published literatures mentioned above, it can be deduced that a quantitative understanding of gas-slag-metal interaction affected by various operation parameters is of significant importance. Detailed work, however, is still needed to further illustrate the interaction process, especially exploring the effect of varying operating parameters and fluid properties.

The objective of the present study is to clarify the interaction behavior between top blown jet and molten steel at various conditions in an 80 t BOF converter. The quantitative effect of operational parameters such as inlet pressure, slag thickness and slag viscosity on the multiphase interaction has been studied. In order to validate the numerical model, water modeling experiments in a scaled-down vessel were performed.

Model Description

Geometrical Model

The components in the model consist of a converter and a lance with converging-diverging nozzles. Liquid steel and slag are contained in the converter with a certain height. The lance is placed above the liquid surface with a specific height in the center position. Table 1 shows the main geometrical dimensions of the converter and top lance and the properties of the materials.

Numerical Assumptions

The computational domain is shown in Fig. 1. The following assumptions have been adopted in order to simplify the simulation:

Table 1 Geometrical dimensions and physical properties of the model

Parameters	Value	Parameters	Oxygen	Steel	Slag
Bath diameter, mm	4020	Density, kg/m ³	Compressible	7100	3500
Bath height, mm	1271	Specific heat, J/(kg·K)	919.31	670	1200
Angle of top lance nozzles, °	12	Thermal conductivity, W/(m·K)	2.46×10^{-2}	40	1.70
nozzles number	4	Surface tension, N/m	–	1.60	0.55
Throat diameter, mm	34.30	Viscosity, kg/(m·s)	Sutherland	0.0065	0.01/ 0.1/0.5

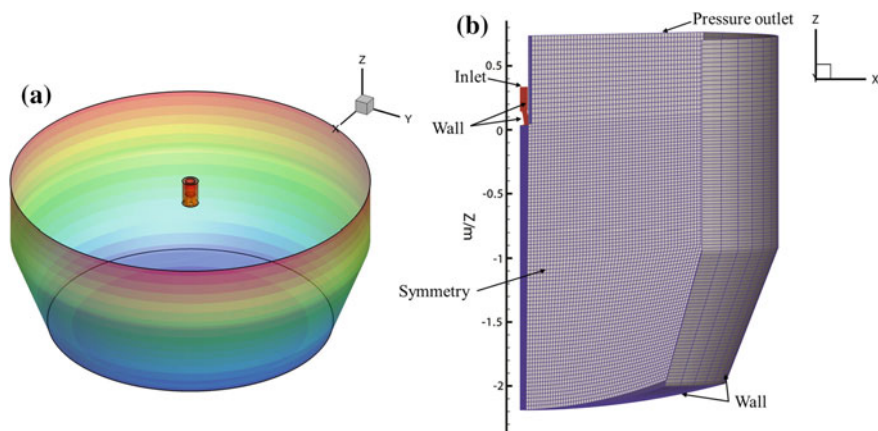


Fig. 1 Schematics of model geometry (a) and mesh system (b)

- (1) The fluids in the converter are treated as Newtonian.
- (2) Chemical reactions are not taken into consideration.
- (3) The flow is symmetric to a vertical plane.
- (4) The physical properties of the molten steel and slag are assumed to be constant.

Governing Equations

The time-dependent motion of the top blown jet and the molten liquid is calculated by the Volume of Fluid (VOF) technique [13]. It is a fixed grid technique designed for tracking the interface between two or more immiscible fluids. In the VOF model, the volume fraction of each phase is tracked throughout the computational domain. In each defined volume, the sum of volume fractions of all phases is unity. The tracking of the interface between the phases is accomplished by the solution of a continuity equation for the volume fraction of one (or more) of the phases. Thus, a single momentum equation shared by all phases is solved, considering the effective density and effective viscosity, which are calculated by a weighted averaging method based on the volume fraction of each phase. Taking the gas phase for example, the continuity, momentum, and energy equations are, respectively, expressed as:

$$\frac{\partial \phi_g}{\partial t} + \mathbf{u} \cdot \text{div} \phi_g = 0 \quad (1)$$

$$\frac{\partial(\rho \mathbf{u})}{\partial t} + \text{div}(\rho \mathbf{u}) = -\text{grad}(p) + \text{div}[\mu_{\text{eff}} \text{grad}(\mathbf{u})] + \rho \mathbf{g} \quad (2)$$

$$\frac{\partial(\rho T)}{\partial t} + \text{div}(\rho \mathbf{u} T) = \text{div}[k_{\text{eff}} \text{grad}(T)] \quad (3)$$

The volume-averaged density and viscosity in each defined volume can be described as:

$$\rho = \rho_g \phi_g + \phi_{st} \rho_{st} + \phi_{sl} \rho_{sl} \quad (4)$$

$$\mu = \mu_g \phi_g + \mu_{st} \phi_{st} + \mu_{sl} \phi_{sl} \quad (5)$$

Where the subscript *g*, *st* and *sl* represent the gas phase, the steel phase and the slag phase, respectively; ϕ is the volume fraction; *t* is time, s; \mathbf{u} is velocity vector, m/s; *p* is the pressure, Pa; μ_{eff} is the effective viscosity coefficient, kg/(m•s); *T* is the temperature, K; k_{eff} is effective thermal conductivity, W/(m•K).

The density of the compressible oxygen is calculated by the ideal gas law equation as follows.

$$\rho_g = \frac{p_{op} + P}{\frac{R}{M_w} T} \quad (6)$$

Where p_{op} is the pressure of the ideal gas, Pa; R is the ideal gas constant, J/(mol·K); M_w is the molecular mass, kg/mol.

Turbulence Model

The standard k - ε model was chosen to describe the turbulence characteristics in this study [14, 15]. Transportation equations of the turbulence kinetic energy k and the dissipation rate ε are respectively given by:

$$\frac{\partial(\rho k)}{\partial t} + \frac{\partial(\rho k u_i)}{\partial x_i} = \frac{\partial}{\partial x_j} \left[\left(\mu + \frac{\mu_t}{\sigma_k} \right) \frac{\partial k}{\partial x_j} \right] + G_k + G_b - \rho \varepsilon - Y_M + S_k \quad (7)$$

$$\frac{\partial(\rho \varepsilon)}{\partial t} + \frac{\partial(\rho \varepsilon u_i)}{\partial x_i} = \frac{\partial}{\partial x_j} \left[\left(\mu + \frac{\mu_t}{\sigma_\varepsilon} \right) \frac{\partial \varepsilon}{\partial x_j} \right] + C_{1\varepsilon} \frac{\varepsilon}{k} (G_k + C_{3\varepsilon} G_b) - C_{2\varepsilon} \rho \frac{\varepsilon^2}{k} + S_\varepsilon \quad (8)$$

Where u_i is the velocity of the fluid in i direction, m/s; G_k is the turbulent kinetic energy generated by average velocity, J; μ_t is the turbulent viscosity, Pa·s; G_b is the turbulent kinetic energy generated by buoyancy, J; Y_M is the turbulent dissipation rate generated by compressible turbulent pulsation; σ_k and σ_ε are the turbulent Prandtl number of k and ε (1.0, 1.3); S_k and S_ε are user-defined source terms; $C_{1\varepsilon}$, $C_{2\varepsilon}$ and $C_{3\varepsilon}$ are empirical constants, which are 1.44, 1.92, 0.09, respectively [16].

Numerical Method

Due to the symmetry of the converter geometry and the flow, only a quarter of the model was adopted as the computational domain and all the boundaries of the computational domain are shown in Fig. 1b.

These unsteady calculations were implemented in FLUENT 16.2. Regarding to the spatial discretization, the Pressure Staggering Option (PRESTO!) scheme and second order upwind scheme were used for pressure and momentum discretization, respectively. The pressure-velocity coupling was achieved by using Pressure Implicit with Splitting of Operators (PISO) algorithm. In addition, the compressive interface-capturing scheme for arbitrary meshes (CICSAM) scheme was adopted. Due to the high speed oxygen jet, the initial time step size adopted in the present simulation was 1×10^{-6} s.

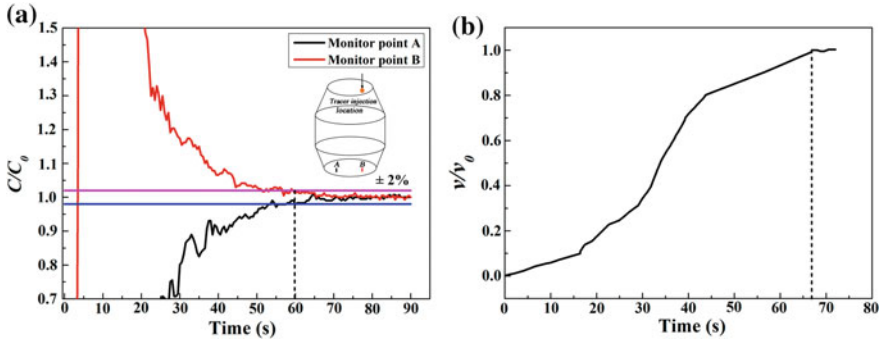


Fig. 2 Comparison of mixing time between physical (a) and mathematical (b) model (c and v are the instantaneous tracer concentration and velocity of the monitored point, the subscript o represents the final value)

The simulations were uploaded to a High Performance Computing (HPC) cluster. 2–5 nodes with 40–100 processors were required for the simulations. The calculations lasted about 40 days.

Model Validation

In order to validate the simulation, water modelling experiments were conducted in a 1/6th scaled-down converter. In the experiments, water, vegetable oil and compressed air were used to simulate molten steel, slag and top blown oxygen, respectively. Detailed information was described in the previous work [17, 18]. The multiphase interaction was evaluated by mixing time in the liquid bath. The simulated and measured mixing times under the present conditions were compared as displayed in Fig. 2. The mixing time measured by water modeling in Fig. 2a is approximately 60 s. The corresponding value obtained from simulation is around 65 s, which is 5 s longer than that of the experimental value. This deviation may be caused by that the tracer injection using a long tube can accelerate the mixing process to some extent and by the errors involved in both simulation and experimentation. Based on the results in Fig. 2, it can be concluded that the computational model is essentially valid in this study.

Results and Discussion

Cavity Formation

During the BOF steelmaking process, a high-pressure supersonic jet impinges on the molten bath and then is deflected upwards. A cavity is generated and metal

droplets are torn from the cavity surface due to the shearing action [19]. Many metallurgical reactions occur during this emulsion process. A fundamental understanding of the cavity formation is an essential aspect for process optimization and it is well worth being investigated.

Figure 3 shows the simulated dynamic interaction between gas and molten slag/steel. The top blown oxygen jet firstly opens the slag layer when the jet strikes the bath surface. The jet gradually pushes the slag away and then an open eye of liquid metal appears. Finally, the oxygen meets the liquid metal. During the process, the cavity is unstable in nature and oscillates both vertically and horizontally, which means the interaction has noticeably instantaneous characteristics. The BOF has an extremely high refining rate partly because of the increased interfacial area created by the high jet momentum [20]. It is estimated that 75–80 wt. pct. of the carbon is removed in the jet impact zone [21].

In addition, surface waves are found inside the cavity. At the beginning of blowing ($t < 0.5$ s), the liquid bath surface is stable and even. Gradually, slag splashing appears ($t = 1$ s) and the cavity is formed on the surface of liquid metal. Meanwhile, the waves in the cavity are pushed by the high speed oxygen jet and morphed into a splash sheet at the margins of the cavity ($t = 1.5$ s). Then, the waves are transmitted to the peripheral slag interface ($t = 3$ s). Correspondingly, it accelerates the interface instability and its irregularity as shown in Fig. 3. Similar phenomena were observed by water modeling experiment [22]. However, the magnitude of the cavity oscillation is closely related to the operation parameters and it will be discussed in the following section.

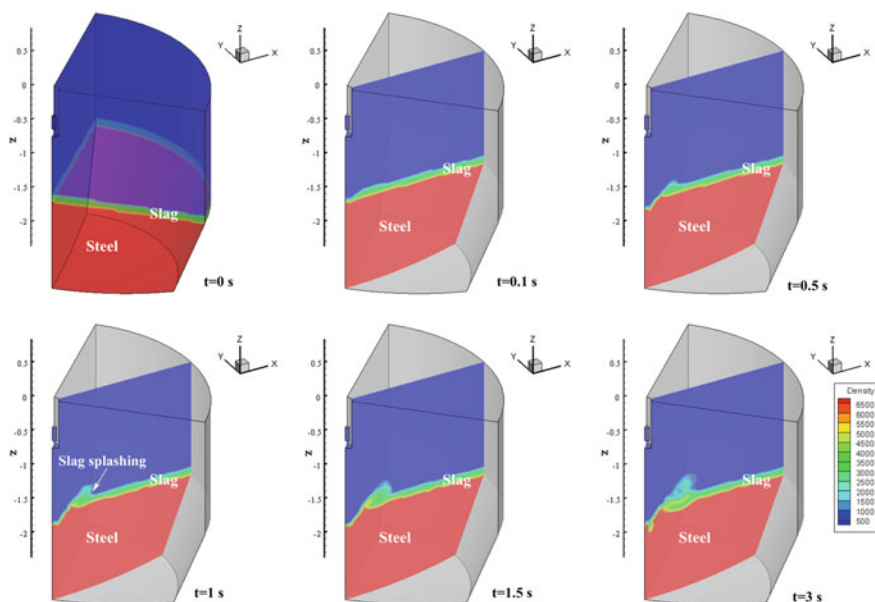


Fig. 3 Gas-slag-metal interaction process

Momentum Characteristics

The gas-slag-steel interaction generates a shaped cavity, which has been proved to be a prerequisite for an uniform mixing and rapid smelting process [23]. Therefore, it is necessary to clarify the interaction behavior, which was affected by different operational parameters. The interaction momentum characteristics under different conditions were assessed at a specific lance height of 950 mm.

Effect of Inlet Pressure

The velocity and turbulence kinetic energy attenuation with initial inlet pressure of 0.7, 0.8, 0.9 and 1.0 MPa, are presented respectively in Fig. 4.

The injected momentum is increased with increasing inlet pressure, which is clearly shown both in the attenuation of velocity and turbulence kinetic energy at given slag properties (Fig. 4). Increasing inlet pressure can introduce more energy to the impact zone, resulting in an intense interaction. Besides, the attenuation of velocity is suppressed with the increase of the inlet pressure. For the interaction area, the velocity with a higher inlet pressure, e.g. 1.0 MPa, almost doubles that at 0.7 MPa (see the zoom-in part in Fig. 4). Consequently, the gas-slag-metal interaction generates a deeper cavity with higher inlet pressure. On the other hand, significant variation of the cavity width in the radial direction under different inlet pressures is not observed. Similar results were found from experimental tests [24].

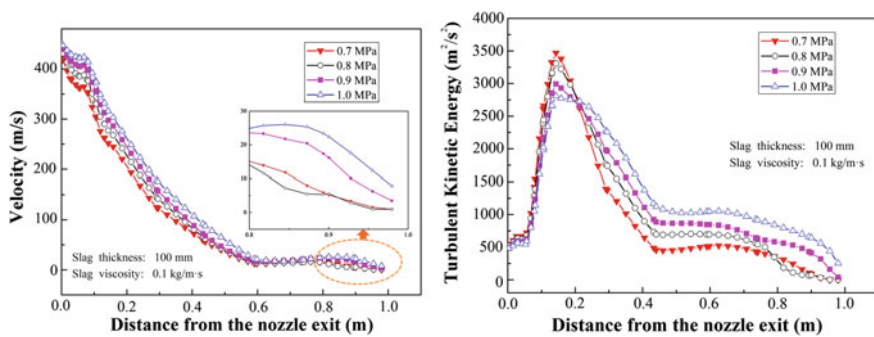


Fig. 4 Attenuation of velocity and turbulence kinetic energy along the injected axis with various pressures

Effect of Slag Thickness

The influence of slag layer was studied since it is important for the gas-slag-steel interaction.

The effect of slag thickness on the interaction momentum is illustrated in Fig. 5. The attenuation tendency of the turbulence kinetic energy is consistent with that of the velocity at different slag thickness. The presence of slag dampens the velocity in the interfacial region as can be seen in the conditions with initial slag thickness of 100 and 150 mm (see the zoom-in part in Fig. 5). The interaction with less slag leads to a deeper cavity. It can also be concluded that the turbulence kinetics energy is very unstable in the area above the interaction zone between gas and liquid slag/steel. The reason can be attributed to the reflection of the oxygen gas. The gas phase is reflected back when the gas interacts with molten slag/steel at higher bath level with thicker slag. Therefore, it can be imagined that turbulence in the adjacent area above the interaction zone is more violent with more slag as indicated in the attenuation of turbulence kinetic energy.

Effect of Slag Viscosity

During steelmaking process, the viscosity of the slag varies with the temperature and slag compositions. To some extent, the variation of slag viscosity can be one or two order of magnitudes [23]. In this context, the gas-slag-metal interaction with varying slag viscosities was numerically investigated.

In Fig. 6, the velocity and turbulence kinetic energy are depicted along the injected axis. Different slag viscosities produce non-significant changes in the attenuations of velocity and turbulent kinetic energy under the given conditions. The penetration depths are almost the same with different viscosities. Only slight turbulence changes can be seen above the interaction zone. Similar conclusions

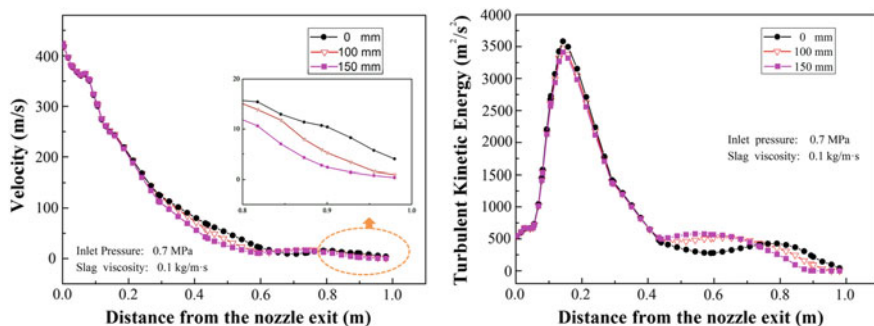


Fig. 5 Attenuation of velocity and turbulence kinetic energy along the injected axis with various slag thicknesses

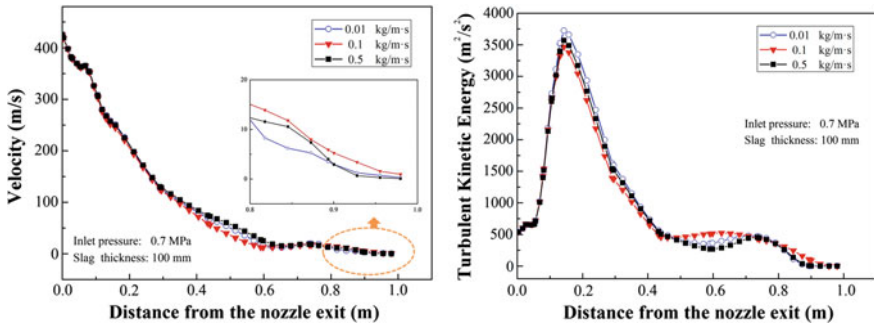


Fig. 6 Attenuation of velocity and turbulence kinetic energy along the injected axis with various slag viscosities

were obtained in the studies of supersonic injection system in electric arc furnace by Memoli et al. [25]. However, further studies are needed to investigate the influence of viscosities with larger order of magnitude variation and of the chemical reactions, which are extremely important in actual production.

Conclusions

The gas-slag-metal interaction during steelmaking of an 80 t BOF converter was investigated by means of VOF approach. The numerical model was validated by water modeling experiment. The findings from the present study can be summarized as follows:

1. The gas-slag-metal interaction has noticeably instantaneous characteristics, and the surface wave in the interaction cavity accelerates the instability and irregularity of the interface.
2. The cavity depth generated from gas-slag-metal interaction increases with increasing inlet pressure, whereas the cavity width is much less affected.
3. The presence of slag dampens the velocity in the interfacial region and thicker slag results in smaller cavity depth.
4. The effect of slag viscosity on the gas-slag-metal interaction is non-significant under the present simulation conditions.

Acknowledgements The financial support from Ministry of Education of the People's Republic of China (No. 20120006110036), Jiangxi Provincial Department of Science and Technology (S2017ZPYFE0263) and computer support from HPC (KU Leuven) are highly acknowledged. Lingling Cao and Yannan Wang want to thank the support of the China Scholarship Council.

References

1. Higuchi Y, Tago Y (2000) Effect of top and bottom blowing conditions on metallurgical characteristics in converter. *Tetsu-to-Hagané* 86(10):654–659
2. Chattopadhyay K (2014) Importance of fluid flow and heat transfer modeling for understanding ironmaking and steelmaking processes. *AIST Trans* 11(3):277–290
3. Emi T (2015) Steelmaking technology for the last 100 years: toward highly efficient mass production systems for high quality steels. *ISIJ Int* 55(1):36–66
4. Szekely J, Evans JW, Brimacombe JK (1988) The mathematical and physical modeling of primary metals processing operations. Wiley, New York
5. Sharma SK, Hlinka JW, Kern DW (1977) The bath circulation, jet penetration and high-temperature reaction zone in BOF steelmaking. *Iron Steelmak.* 4:7–18
6. Molloy NA (1970) Impinging jet flow in a 2-phase system-basic flow pattern. *J Iron Steel Inst* 208:943–950
7. Nordquist A, Kumbhat N, Jonsson L et al (2006) The effect of nozzle diameter, lance height and flow rate on penetration depth in a top-blown water model. *Steel Res Int* 77(2):82–90
8. Odenthal HJ, Falkenreck U, Schlüter J (2006) CFD simulation of multiphase melt flows in steelmaking converters. European conference on computer fluid dynamics, Egmond aan Zee, The Netherlands, 5–8 September 2006
9. Li Q, Li MM, Kuang SB et al (2015) Numerical simulation of the interaction between supersonic oxygen jets and molten slag–metal bath in steelmaking BOF process. *Metall Mater Trans B* 46(3):1494–1509
10. Sabah S, Brooks G (2016) Study of cavity modes in BOF by analysis of sound. *Ironmak Steelmak* 43(6):473–480
11. Wang Z, Liu Q, Xie FM et al (2012) Model for prediction of oxygen required in BOF steelmaking. *Ironmak Steelmak* 39(3):228–233
12. Liu FH, Zhu R, Wang QG et al (2015) Simulation and application of top lance with various tilt angles in dephosphorization ladle furnace. *ISIJ Int* 55(8):1633–1641
13. Welch SW, Wilson J (2000) A volume of fluid based method for fluid flows with phase change. *J Comp Phys* 160(2):662–682
14. Asahara N, Naito K, Kitagawa I et al (2011) Fundamental study on interaction between top blown jet and liquid bath. *Steel Res Int* 82(5):587–594
15. Wang WJ, Yuan ZF, Matsuura H et al (2010) Three-dimensional compressible flow simulation of top-blown multiple jets in converter. *ISIJ Int* 50(4):491–500
16. Launder BE, Spalding DB (1972) *Mathematical models of turbulence*. Academic Press, London
17. Cao LL, Wang Z, Liu Q et al (2015) Physical modeling research on the stirring characteristics and mixing effect of an 80 t converter. The 6th International Congress on the Science and Technology of Steelmaking, Beijing, China, 12–14 May 2015
18. Cao LL, Liu Q, Wang Z et al (2016) Interaction behaviour between top blown jet and molten steel during BOF steelmaking process. *Ironmak Steelmak* . <https://doi.org/10.1080/03019233.2016.1255373>
19. Deo B, Boom R (1993) *Fundamentals of steelmaking metallurgy*. Prentice-Hall, New York
20. Meyer HW, Porter WF, Smith GC et al (1968) Slag-metal emulsions and their importance in BOF steelmaking. *J Met* 20(7):35–42
21. Price DJ (1974) *Process engineering of pyrometallurgy*. Institution of Mining and Metallurgy London, UK
22. Sabah S, Brooks G (2014) Splashing in oxygen steelmaking. *ISIJ Int* 54(4):836–844

23. Yuan ZF, Pan DF (2007) Oxygen lance technology for steelmaking. Metallurgical Industry Press, Beijing, China
24. Cheslak FR, Nicholls JA, Sichel M (1969) Cavities formed on liquid surfaces by impinging gaseous jets. *J Fluid Mech* 36(1):55–63
25. Memoli F, Mapelli C, Ravanelli P et al (2004) Simulation of oxygen penetration and decarburisation in EAF using supersonic injection system. *ISIJ Int* 44(8):1342–1349